

# Comparative Study of Thermally Sprayed Coatings Under Different Types of Wear Conditions for Hard Chromium Replacement

Š. Houdková · F. Zahálka · M. Kašparová ·  
L.-M. Berger

Received: 12 January 2011 / Accepted: 22 April 2011 / Published online: 8 May 2011  
© Springer Science+Business Media, LLC 2011

**Abstract** The tribological properties of part surfaces, namely their wear resistance and friction properties, are decisive in many cases for their proper function. To improve surface properties, it is possible to create hard, wear-resistant coatings by thermal spray technologies. With these versatile coating preparation technologies, part lifetime, reliability, and safety can be improved. In this study, the tribological properties of the HVOF-sprayed coatings WC–17%Co, WC–10%Co4%Cr, WC–15% NiMoCrFeCo, Cr<sub>3</sub>C<sub>2</sub>–25%NiCr, (Ti,Mo)(C,N)–37%NiCo, NiCrSiB, and AISI 316L and the plasma-sprayed Cr<sub>2</sub>O<sub>3</sub> coating were compared with the properties of electrolytic hard chrome and surface-hardened steel. Four different wear behavior tests were performed; the abrasive wear performance of the coatings was assessed using a dry sand/rubber wheel test according to ASTM G-65 and a wet slurry abrasion test according to ASTM G-75, the sliding wear behavior was evaluated by pin-on-disk testing according to ASTM G-99, and the erosion wear resistance was measured for three impact angles. In all tests, the HVOF-sprayed hardmetal coatings exhibited superior properties and can be recommended as a replacement for traditional surface treatments. Due to its tendency to exhibit brittle cracking, the plasma-sprayed ceramic coating Cr<sub>2</sub>O<sub>3</sub> can only be recommended for purely abrasive wear conditions. The tested HVOF-sprayed metallic coatings, NiCrSiB and AISI 316L, did not have sufficient wear

resistance compared with that of traditional surface treatment and should not be used under more demanding conditions. Based on the obtained data, the application possibilities and limitations of the reported coatings were determined.

**Keywords** Thermal spray coatings · HVOF · Hardmetals · Wear testing · Hard chrome replacement

## 1 Introduction

The wear resistance of functional surfaces is the critical factor for many machine parts in industrial applications. The most widespread commercially used surface treatment, aimed to ensuring the surface's wear and corrosion resistance, is functional hard chrome plating. The main disadvantage of hard chrome plating technology is the presence of health-endangering and environmentally problematic hexavalent chromium in the plating bath [1–3]. For this reason, the use of hard chrome plating technology is subject to increasingly strict rules and restrictions, which make it more challenging and costly [4]. One possible solution is the replacement of traditional surface treatment by thermally sprayed wear-resistant coatings. A wide range of materials can be processed using predominantly plasma, flame, and electric arc spraying for a wide variety of applications ranging from gas turbine technology to the electronics industry. For creation of hard, wear-, and corrosion-resistant coatings, the most suitable materials are ceramics and hardmetals. Plasma spraying is used for spraying the ceramics, due to their high melting points. The high velocity oxy-fuel (HVOF) spraying technology is usually selected for the deposition of high-quality hardmetals and metals coatings [5].

Š. Houdková (✉) · F. Zahálka · M. Kašparová  
University of West Bohemia, Univerzitní 8,  
306 14 Plzen, CZ, Czech Republic  
e-mail: houdkov@ntc.zcu.cz

L.-M. Berger  
Fraunhofer Institute for Materials and Beam Technology  
(Fh-IWS), Winterbergstrasse 28, 01277 Dresden, Germany

Up to now, many studies have focused on comparison of tribological properties of thermally sprayed coatings and hard chrome plating, e.g. [6–11]. The most detailed studies on hard chromium replacement by HVOF-sprayed coatings for aircraft applications were conducted in the US-Canadian HCAT program [12]. Tungsten carbide (WC)- and chromium carbide ( $\text{Cr}_3\text{C}_2$ )-based hardmetals sprayed by HVOF [7–10, 12] are the most commonly recommended coating materials. Nevertheless, given the higher cost of the HVOF technology and for some particular wear conditions, plasma-sprayed  $\text{Cr}_2\text{O}_3$  coatings are also recommended [6, 9]. To protect the coated parts against corrosion, the bond coat preventing the corrosive solution to interact directly with the metallic substrate are often used, even if the ceramic thermal spray coatings are often corrosion resistant as far as the coating material are concerned (Al, Cr, etc.) [13, 14]. Comparing the benefits and costs of the evaluated coatings, not only the service performance should be considered [15]. The hard chrome coating process demands more complicated and time-spending preparation operations, such as rinsing, etching, masking and so on. On the other hand, the hard chrome coating process itself is cheaper. The costs of thermal spray strongly depend on used coatings material. Applying the superior hard phase containing coatings such as hard metals, the further costs has to be taken into account connected with the final surface finishing that has to be usually achieved by expensive diamond tools.

The objective of this study is to compare the behavior of one experimental and several commercially available materials suited for wear-resistant application under different wear conditions. The wear resistance, coefficient of wear and the wear mechanism are investigated. Even if there are many wear studies of thermally sprayed coatings, they are usually concentrated on particular wear conditions. The presented comparison, supported by extensive amount of measured data, enables to evaluate credibly the applicability of the most frequently used surface treatments with respect to different working conditions.

## 2 Materials and Methods

### 2.1 Materials and Coating Preparation

In this study, seven commercial coating materials and one experimental material were investigated in terms of their ability to resist abrasive wear in different wear conditions. A hard chrome coating and hardened steel were also evaluated for comparison purposes. The HVOF-sprayed coatings were deposited on grit-blasted mild steel substrates using HP/HVOF JP-5000<sup>®</sup> (TAF A) spray equipment at VZU Plzeň Ltd. in Pilsen, Cz. Details of the spraying parameters and procedures employed in the spraying of the coatings can be found in Table 1. The equivalent ratio, introduced in Table 1, is defined as the ratio of the mass of fuel divided by the mass of oxygen used for spraying to the stoichiometric ratio of fuel and oxygen:

$$\Phi = \frac{F/O}{\left(\frac{F}{O}\right)_{st}} \quad (1)$$

where F stands for fuel (kerosene in this case) and O stands for oxygen.

The  $\text{Cr}_2\text{O}_3$  coatings were prepared by plasma spraying using the F4 Sulzer Metco gun. A NiCr coating 50  $\mu\text{m}$  in thickness was used as a bond coat. Deposition parameters are shown in Table 2. For the steel hardening, the substrate was first heated to 840  $^{\circ}\text{C}$  and held for 15 min, then cooled in oil to 160  $^{\circ}\text{C}$  and held for 2 h, and finally cooled in air. The hard chrome coating was prepared at BUZULUK Inc. in Komárov, Cz., using the standard procedure.

Prior to wear testing, the coatings and hardened steel were evaluated in terms of their mechanical properties. The measured mechanical properties are summarized in Table 3. The coating thickness was measured on the coating cross-section and the surface roughness Ra on as-sprayed surfaces. The apparent density of the coating was determined according to Archimedes' law from the weight of the sample measured in water and in air. The HV0.1 microhardness was measured on the coating cross-section,

**Table 1** Deposition parameters for HVOF coatings

Coating	Powder trade name	Equivalent ratio	Carrier gas	Barell length (mm)	Spray distance (mm)
WC–17%Co	FST K-674.23	0.8	Argon	150	380
WC–10%Co4%Cr	FST K-647.23	0.8	Argon	150	380
WC–15%Hastelloy	AMPERIT 529.074	0.8	Argon	150	380
$\text{Cr}_3\text{C}_2$ –25%NiCr	1375VM	0.8	Argon	150	360
(Ti,Mo)(C,N)–18.5%Ni18.5%Co	Experimental powder	1	Argon	150	380
NiCrSiB	FST M-771.33	0.8	Argon	100	360
AISI 316L	FST M-684.33	0.8	Nitrogen	100	360

**Table 2** Deposition parameters for plasma-sprayed coatings

Coating	Powder supplier and trade name	Argon (L/min)	Hydrogen (L/min)	Argon carrier gas (L/min)	Current (A)	Spray distance (mm)
NiAl	Porex	55	9.5	3.5	600	140
Cr <sub>2</sub> O <sub>3</sub>	Wirpo, GTV 40.06.7	40	13	3.6	650	120

**Table 3** Coating properties

Coating	Thickness (μm)	As-sprayed surface roughness Ra (μm)	Polished surface roughness Ra (μm)	Apparent density (g cm <sup>-3</sup> )	Microhardness HV0.1	Hardness HR15N	IFT (MPa m <sup>1/2</sup> )
WC–Co	442 ± 10	2.76 ± 0.02	0.08 ± 0.01	13.16	1240 ± 116	92.7 ± 1.2	2.41 ± 0.46
WC–CoCr	467 ± 9	3.05 ± 0.5	0.07 ± 0.01	13.09	1369 ± 114	92.0 ± 1.0	2.37 ± 0.26
WC–Hastelloy	410 ± 17	3.08 ± 0.02	0.09 ± 0.01	13.25	1167 ± 109	92.8 ± 0.7	0.68 ± 0.17
Cr <sub>3</sub> C <sub>2</sub> –NiCr	433 ± 9	3.85 ± 0.32	0.16 ± 0.04	6.64	786 ± 123	91.0 ± 0.8	1.45 ± 0.47
(Ti,Mo)(C,N)–NiCo	430 ± 7	2.95 ± 0.46	0.08 ± 0.02	6.31	799 ± 131	91.5 ± 1.5	0.5 ± 0.05
NiCrSiB	379 ± 12	7.31 ± 0.79	0.10 ± 0.03	7.30	735 ± 59	89.0 ± 1.6	0.92 ± 0.18
AISI 316L	427 ± 12	9.34 ± 0.87	0.11 ± 0.02	7.80	321 ± 31	54.0 ± 5.4	0.33 ± 0.04
Cr <sub>2</sub> O <sub>3</sub>	490 ± 16	3.32 ± 0.29	0.10 ± 0.03	5.20	962 ± 112	93.2 ± 3.2	0.35 ± 0.03
Hardened steel	–	0.33 ± 0.16	0.05 ± 0.03	7.87	700 ± 89	88.8 ± 0.8	–
Hard chrome	290 ± 31	0.21 ± 0.01	0.05 ± 0.001	7.14	884 ± 97	90.1 ± 1.2	–

and the HR15N surface hardness was measured on the top of the as sprayed coating using a Rockwell cone indenter with a load of 15 kg. With respect to the coatings thickness, the used load of 15 kg precludes the influence of substrate properties on measured values. While the microhardness measurement refers to the inner properties of coating material, the surface hardness measurement brings information about the overall coating properties, including porosity, intersplat cohesion, etc. More to that, the orientation of indentation with respect to the coatings strongly anisotropic microstructure also plays its role. The results of surface hardness and microhardness cannot be directly compared.

The indentation fracture toughness (IFT) was determined from the lengths of the cracks emanating from the corners of the Vickers indentation made in the coating cross-section at a force of 200 N. The method of indentation fracture toughness evaluation is described in detail by Ponton et al. in the literature [16, 17], where 19 formulas for IFT are discussed. Their application on measured coatings results in different values of IFT, but the general trend is the same [18]. The values of IFT presented in this study were determined according to the Lawn and Fuller formula [19]:

$$K_c = 0.0515 \left( \frac{L}{ac^{3/2}} \right) \quad (2)$$

where  $K_c$  is the fracture toughness determined from the indentation tests,  $L$  the indenter load,  $a$  the half-length of the indentation diagonal, and  $c$  is the total crack length, defined as the average of two crack lengths plus the half-length of the indentation diagonal.

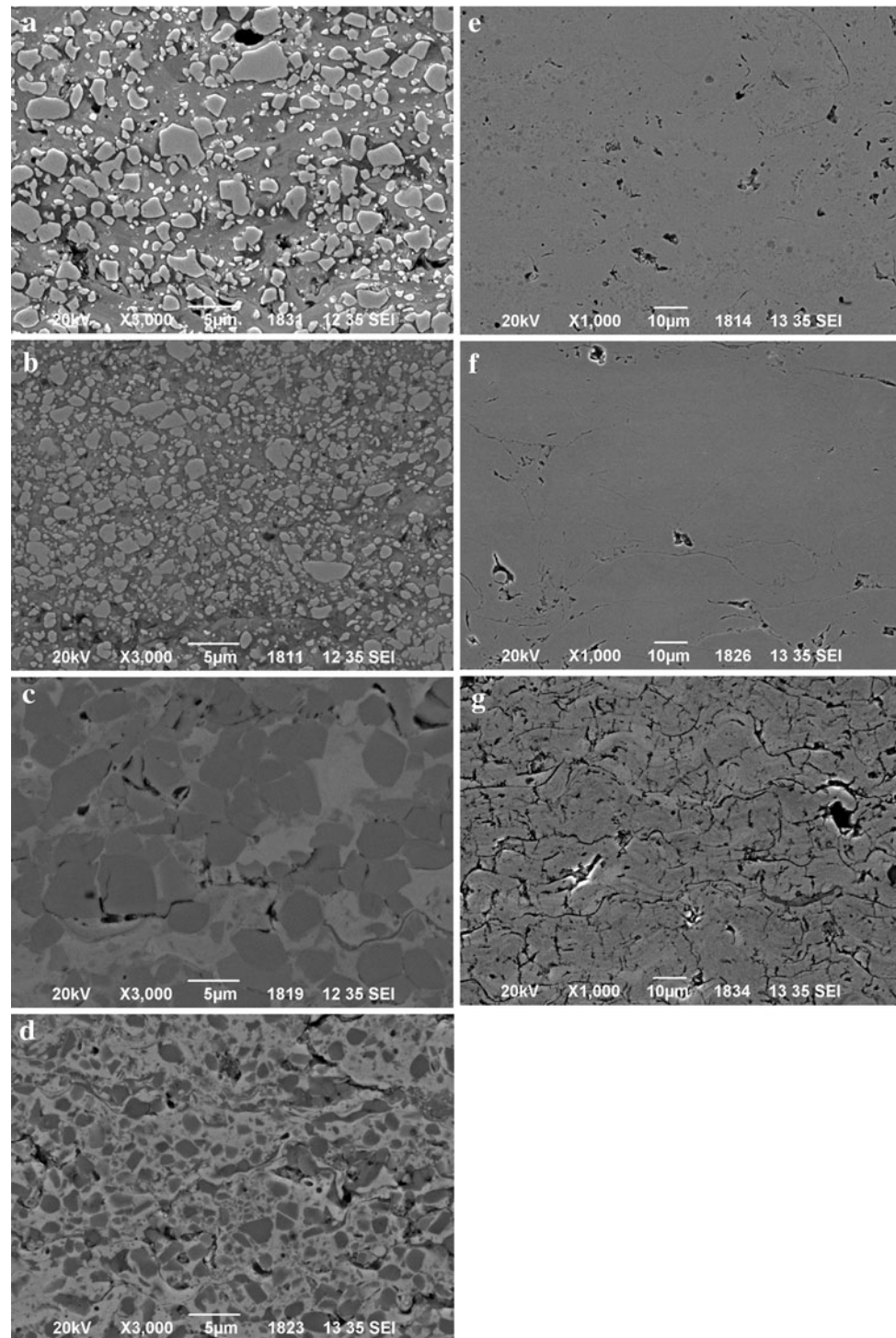
The very low IFT values of metallic AISI 316L and NiCrSiB coating were caused by the low intersplat cohesion of the two coatings. In the case of AISI 316L, the cohesion was decreased by oxides originating during spraying on the splat boundary; in the case of the NiCrSiB coating, the mechanical properties were lower than expected due to the missing thermal posttreatment that is commonly used to improve coatings microstructure and properties [20].

The SEM images of the coating microstructures are given in Fig. 1. A detailed microstructural study of hardmetal coatings was published elsewhere [21]. The phase compositions of the hardmetal coatings sprayed under analogous conditions are discussed in another article [22].

## 2.2 Wear Tests

Four wear tests were performed for the purposes of comparing the tribological properties of the coatings. The 3-body abrasive wear tests provided information about

**Fig. 1** Microstructures of  
**a** WC–Co coating,  
**b** WC–Hastelloy coating,  
**c** Cr<sub>3</sub>C<sub>2</sub>–NiCr coating,  
**d** (Ti,Mo)(C,N)–NiCo coating,  
**e** NiCrSiB coating,  
**f** AISI 316L coating, and  
**g** Cr<sub>2</sub>O<sub>3</sub> coating

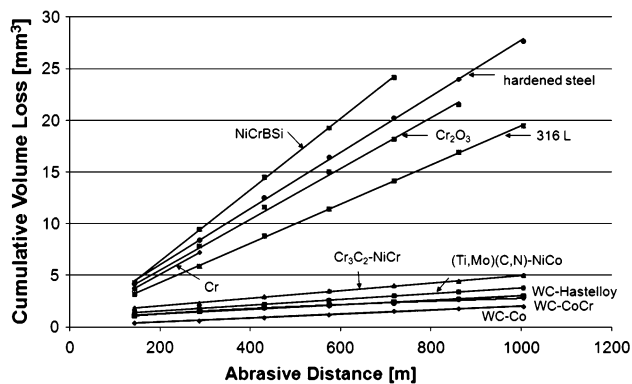


abrasive wear rate and mechanism under dry (sand rubber wheel test) and wet (slurry test) conditions [23, 24]. The unidirectional sliding wear pin-on-disk test, performed by means of a CSEM Instruments High Temperature Tribometer [23], enabled to measure the coefficient of friction for two kinds of counterparts materials—Al<sub>2</sub>O<sub>3</sub> and steel.

The erosive wear was evaluated at ATG Ltd. in Prague, CZ by means of a centrifugal accelerator, described by Kleis et al. [25], using three different angles of particle impingement for evaluation of the effect of impingement angle on wear rate and mechanism. The parameters used for wear testing are summarized in Table 4.

**Table 4** Test parameters

Parameter	Dry abrasion	Wet abrasion	Pin-on-disk	Erosion
Test standard	ASTM G-65	ASTM G-75	ASTM G-99	–
Abrasive media	Al <sub>2</sub> O <sub>3</sub> , particle size (212–250 μm) flow rate 440 g/min	50 wt% Al <sub>2</sub> O <sub>3</sub> , particle size (60–90 μm) with 50 wt% water	Al <sub>2</sub> O <sub>3</sub> ball Steel ball 6 mm diameter	Casting sand, 1000HV, particle size 0.8 mm
Test loads	22 N	20 N	10 N	50 m/s impact velocity
Sliding speed	–	–	0.1 m/s	–
Test distance (cycles)	1,005 m	9,216 m	50,000 cycles	5 kg of abrasive media
Mass loss measurement	283 m intervals	2,304 intervals	At the end of the test	At the end of the test
Number of specimens	3	4	3	3
Specimen dimensions	(76 × 25 × 5) mm	(25 × 15 × 10) mm	25 mm dia. × 5 mm	(20 × 15 × 4) mm
Specimen preparation	As-sprayed	As-sprayed	Polished to Ra given in Table 3	As-sprayed

**Fig. 2** Dry abrasion wear results—total volume loss

### 3 Results and Discussion

#### 3.1 Dry Sand/Rubber Wheel Abrasion Test

The results of the dry sand/rubber wheel (DSRW) abrasion test for all tested materials are shown in Fig. 2. It

represents the cumulative volume loss of coating material versus the abrasive distance. In addition, the linear wear rate  $W_r$  (mm<sup>3</sup>/m) was determined from a linear fit of the cumulative wear loss and abrasive distance dependence (Fig. 2), and the coefficient of abrasive wear resistance  $K_{abr}$  (mm<sup>3</sup>/Nm) was calculated according to:

$$K_{abr} = \frac{V}{Ll} \quad (3)$$

where  $V$  is the cumulative wear loss (mm<sup>3</sup>),  $L$  is the load (N), and  $l$  is the abrasive distance (m).

The values for total volume loss, wear rate, and wear coefficient can be found in Table 5.

The test was performed with an abrasive distance of 1,005 m, except for NiCrBSi, where the substrate material was revealed at an abrasive distance of 718 m, and the hard chrome coating, where it occurred at an abrasive distance of 287 m. The initial thicknesses of these two coatings were the lowest and the abrasive medium used, highly effective sharp-edged Al<sub>2</sub>O<sub>3</sub>, was chosen for testing of wear-resistant hardmetal coatings and is not the most

**Table 5** Results of dry sand/rubber wheel abrasion test

Coating	Abrasive distance (m)	Total volume loss (mm <sup>3</sup> )	Linear wear rate (mm <sup>3</sup> /m)	Coeff. of wear resistance $K_{abr}$ (mm <sup>3</sup> /Nm)
WC-Co	1,005	1.91 ± 6.08E-02	2.00E-03	9.00E-05 ± 2.75E-06
WC-CoCr	1,005	2.81 ± 4.00E-02	2.10E-03	1.27E-04 ± 5.01E-04
WC-Hastelloy	1,005	2.96 ± 8.66E-02	2.00E-03	1.34E-04 ± 4.97E-04
Cr <sub>3</sub> C <sub>2</sub> -NiCr	1,005	4.50 ± 1.15E-01	3.80E-03	2.04E-04 ± 5.22E-06
(Ti,Mo)(C,N)-NiCo	1,005	3.40 ± 3.46E-02	2.90E-03	1.54E-04 ± 1.57E-06
NiCrSiB	718	24.14 ± 7.21E-02	3.45E-02	1.53E-03 ± 4.57E-06
AISI 316L	1,005	19.46 ± 1.59E-01	1.90E-02	8.804E-04 ± 7.18E-06
Cr <sub>2</sub> O <sub>3</sub>	862	21.49 ± 1.15E-02	2.45E-02	1.13E-03 ± 6.09E-07
Hardened steel	1,005	27.67 ± 4.62E-02	2.72E-02	1.25E-03 ± 2.09E-06
Hard chrome	287	7.21 ± 1.2E-02	2.46E-02	1.14E-03 ± 6.52E-07



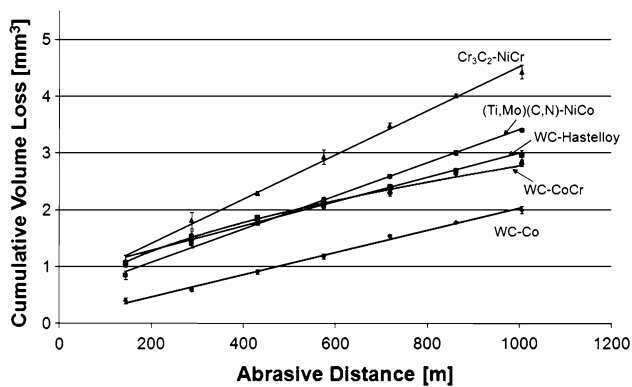


**Fig. 3** Dry abrasion wear results for hardmetal coatings—total volume loss

suitable abrasive for testing of softer coatings. In this case, it was used to standardize the study and made the comparison with hardmetal coatings possible. The effect of the abrasive particle material on wear of HVOF coatings has been studied elsewhere [26].

As can be seen in Fig. 2, the coatings can be divided into two groups. The first group is formed by the hardmetal coatings with high wear resistance. The non-hardmetal coatings, which form the second group, exhibited a volume loss that was several times higher during testing.

For the hardmetal coatings, the results are shown in more detail in Fig. 3. The highest wear resistance was measured for WC-based coatings. The differences were very small, as were the differences between the hardness values (see Table 3). The hardness values can be influenced by a number of parameters, including amount of porosity, carbide content, size and shape, extent of phase transformation during spraying, etc. [27]. The WC-based coatings had the highest hardness values of all coatings investigated in this study. However, from hardness values alone conclusions on the abrasion wear behavior cannot be drawn [28]. Also the size and distribution of hard particles and their bond to the surrounding matrix play its role, as it can be seen from the results below.

The (Ti,Mo)(C,N)-NiCo coating also showed excellent abrasion wear resistance. In this type of material, core-rim structured hard phase particles are embedded in the metallic binder matrix. The microstructure and properties of (Ti,Mo)(C,N)-NiCo coatings are described in detail in the literature [29–33]. The size of the hard phase particles in the (Ti,Mo)(C,N)-NiCo coating is in the range 0.40–3.4  $\mu\text{m}$ . The influence of size and distribution of hard particles in HVOF coatings on the mechanical properties and abrasive wear resistance of the coatings was studied by Miguel et al. [27], Yang et al. [34], and Chivavibul et al. [35]. It was shown that the coatings with lower average hard phase particle sizes had higher wear resistance levels.

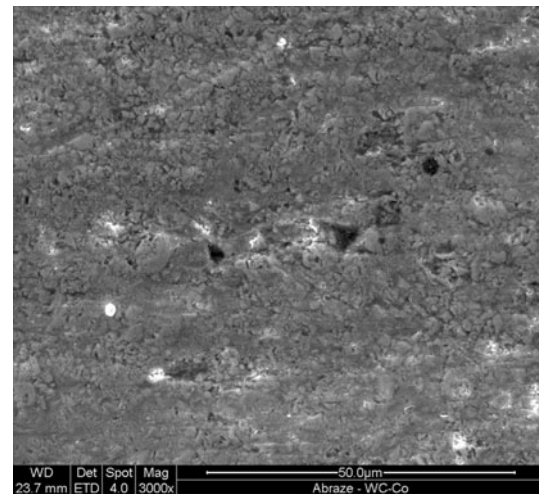


**Fig. 4** Surface of WC-Co coating after dry abrasion wear test

It appears that despite the relative low hardness, the hard phase particle size was advantageous under the given test conditions.

The mechanism of wear was similar for all hardmetal coatings. The worn surface was smooth, with very shallow irregular grooves. The hard particles protected the coatings against deep penetration of abrasive particles and lowered the mean free path of the groove. The major mechanism of wear was connected with removal of the matrix from the areas between the hard particles, followed by weakening of the bonds and pullout from the coating surface (Fig. 4). In the case of the Cr<sub>3</sub>C<sub>2</sub>-NiCr coating, due to the higher porosity, the mechanism of pullout of large coating fragments on the splat boundary was also observed. Together with the lower hardness, the above-described wear mechanism was responsible for the relatively high wear rate of this coating compared with those of other hardmetal coatings.

In the group of non-hardmetal coatings, the highest wear resistance was found for the AISI 316L steel coating. This result was surprising in light of the low hardness and measured IFT of the coating. One of the reasons for this result could be found in the embedding of abrasive particles in the coating surface, possibly leading to an increase in surface wear resistance. The SEM and EDX analyses confirmed the presence of Al<sub>2</sub>O<sub>3</sub> particles in the coating surface (Figs. 5 and 6). The wear scars in the AISI 316L coatings were short and oriented in various ways, indicative of the influence of the embedded Al<sub>2</sub>O<sub>3</sub> particles. The mechanism of increasing the wear resistance by progressive embedding of hard abrasive particles in the coating surface during the wear test in the case of metallic coatings is described in the literature [6, 28]. The other reason could be found in the heavy plastic deformation of the steel coating, not accompanied by material loss. The advantage



**Fig. 5** Surface of AISI 316L coating after dry abrasion wear test (the embedded  $\text{Al}_2\text{O}_3$  particle is labeled “1”, and the coating material is labeled “2”)

of the tendency for plastic deformation is made clear through comparison with the results of the  $\text{Cr}_2\text{O}_3$  coating, which was much harder, but behaved in a brittle manner. Comparison of these two materials leads to the conclusion that the hardness alone is not decisive for the abrasion behavior. Nevertheless, abrasive cutting and scratching can be considered to be a key wear mechanism.

The other non-hardmetal HVOF coating, NiCrSiB, showed the lowest wear resistance. The worn surface was formed by numerous wear scars oriented in the direction of wheel rotation. The sizes and amounts of hard phases, mostly CrB,  $\text{Cr}_7\text{C}_3$ , and  $\text{Ni}_3\text{B}$  [27], in the coating structure

were too small to have a significant influence on coating wear resistance. On the other hand, the coating was too hard to enable the embedding of abrasive particles in the coating surface, as occurred in the AISI 316L coating, so the reinforcement effect did not play a role. The NiCrSiB coating can yield better results if it is heat treated so that hard phases can grow [5].

The microstructure of the plasma-sprayed  $\text{Cr}_2\text{O}_3$  coating differed significantly from those of the HVOF coatings. The high spray temperatures resulted in shrinkage stresses in the coating, which led to the creation of a network of fine (0.1–0.45  $\mu\text{m}$ ) cracks. The lower spraying velocity was responsible for the higher porosity and the higher adhesive strength between individual splats. The worn surface (Fig. 7) was smooth, without signs of wear tracks or plastic deformation. Loss of large coating fragments, caused by brittle cracking of splat boundaries with the help of the existing crack network was identified to be a key wear mechanism. The cyclic stress from abrasive particles may also have played a role, possibly causing fatigue stress. The disposition of  $\text{Cr}_2\text{O}_3$  coating to brittle cracking could be predicted from its high hardness and low fracture toughness (Table 3). A similar wear mechanism was identified by Bolelli et al. [6].

Bolelli [6, 28] persuaded to the conclusion that ceramic coatings are more wear-resistant at the beginning of the test after a low number of disk revolutions due to the high hardness, whereas the embedded particles protect the metallic and hardmetal coatings from further grooving or indenting phenomena after a high number of disk revolutions (longer abrasive distance). Similar behavior was

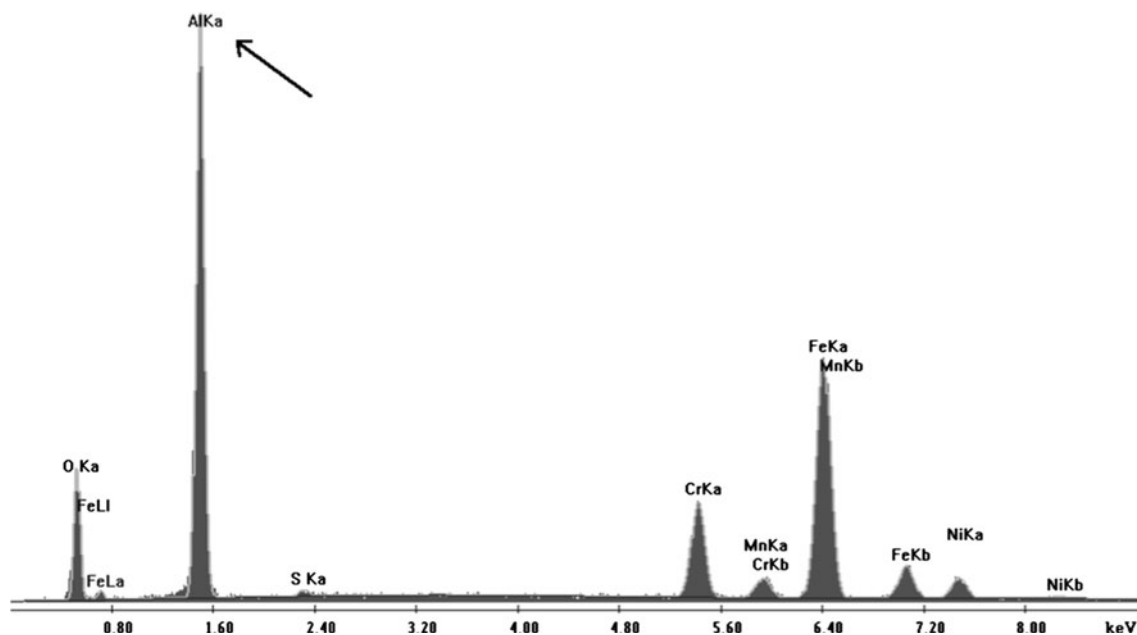


**Fig. 6** EDX analysis of AISI 316L coating surface after dry abrasion wear test

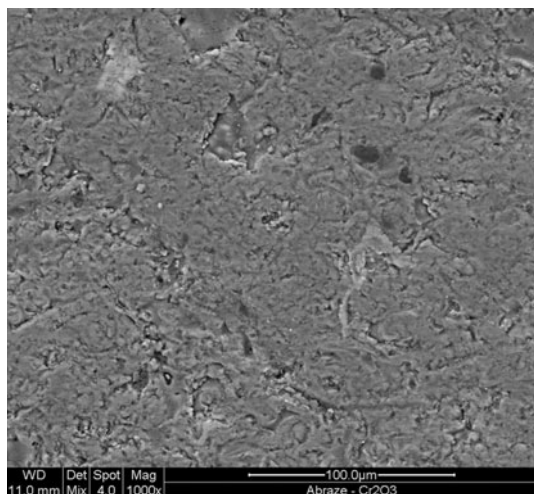


**Fig. 7** Worn surface of  $\text{Cr}_2\text{O}_3$  coating after dry abrasion wear test

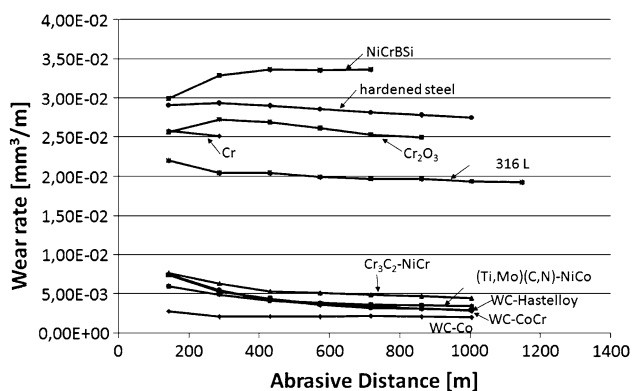


**Fig. 8** Dry abrasion wear results—linear wear rate

observed in this study. It is the linear wear rate  $W_r$  ( $\text{mm}^3/\text{m}$ ) plotted versus abrasive distance (Fig. 8), similarly to the [28], the difference between the hardmetal coatings behavior and the behavior of other coatings is evident. While  $\text{Cr}_2\text{O}_3$ , NiCrBSi, and hardened steel wore out faster with increasing abrasive distance, the hardmetal coatings wore out the most from the beginning of the test. The AISI 316L behaved the same way as hardmetal coatings. This observation confirms the conclusion of embedding the hard abrasive particles to the soft AISI 316 coating, making it more wear resistant.

Compare to the results of [6, 28], there were no embedded particles identified in hardmetal coatings in our case. The differences might be explained by the use of different wheel materials. In the article by Bolelli et al. [6, 28], the wheel was made of steel; in our case, it was rubber, which, being softer, gave the abrasive particles a greater amount of play. The different wheel material led to different stress conditions, and the tests were accordingly called “low” (for a rubber wheel) and “high” (for a steel wheel) abrasion tests.

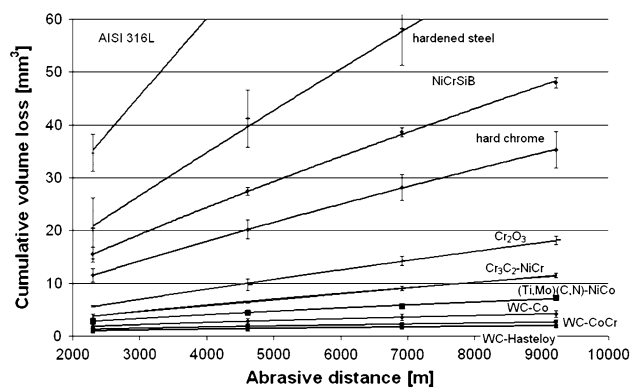


**Fig. 9** Results of wet abrasion wear test

### 3.2 Wet Slurry Abrasion Wear Test

The results of wet slurry abrasion tests for all tested materials are shown in Fig. 9, which illustrates the cumulative volume loss of coating material in dependence on abrasive distance. As for the dry abrasion wear test, for this test, the wear rate  $W_r$  ( $\text{mm}^3/\text{m}$ ) and the linear coefficient of abrasive wear resistance  $K_{abr}$  ( $\text{mm}^3/\text{Nm}$ ) were calculated according to ASTM G-75. The values can be found in Table 6.

Like in the dry abrasion test, in this test, the coatings could be divided into two groups based on the wear results and mechanisms: the HVOF-sprayed hardmetal coatings and the other coatings.

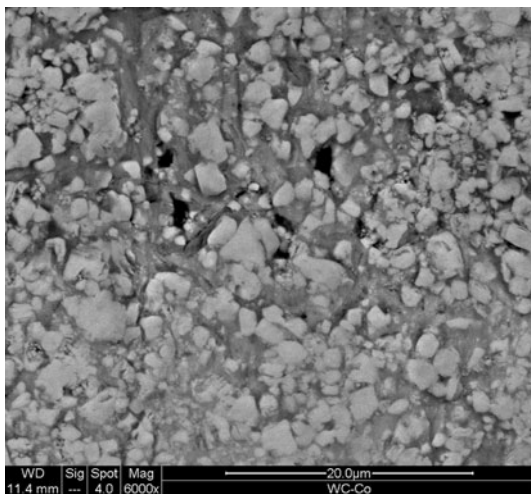
In the case of the wet slurry abrasion test, the abrasive medium was analogous to the medium used for grinding in the process of microstructural sample preparation. The wear mechanism of hardmetal coatings could also be described as microgrinding and polishing. The material loss was observed mainly in the matrix, but the shape of the hard carbides changed from sharp-edged to more rounded as a result of the wear test. The appearance of the worn surface was similar for all WC-based hardmetal coatings (Fig. 10).

The ranking of the WC-based coatings based on wear resistance reflected the influence of corrosion. The lowest wear loss was recorded for the WC–Hastelloy coating, where the matrix was designed to be a highly corrosion-resistant alloy. The WC–Hastelloy coating was followed by the WC–CoCr coating. Compared to WC–Co, the amount of the metallic binder phase is lower, mostly due to formation of secondary carbide phases [36]. In addition, alloying of cobalt with chromium takes place. The WC–Co, characterized by high hardness and indentation fracture toughness, was the last in the group of WC-based coatings. In a article published by Fedrizzi et al. [37], the tribocorrosion behavior of WC and  $\text{Cr}_3\text{C}_2$ -based HVOF hardmetal coatings was studied, although in a sodium



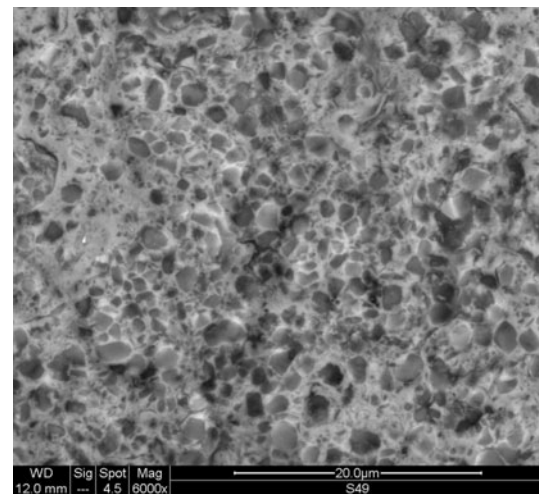
**Table 6** Results of wet slurry abrasion test

Coating	Total volume loss (mm <sup>3</sup> )	Linear wear rate (mm <sup>3</sup> /m)	Coeff. of wear resistance $K_{abr}$ (mm <sup>3</sup> /Nm)
WC–Co	4.162 ± 0.622	2.25E–04 ± 0.40E–04	2.25E–05 ± 3.38E–06
WC–CoCr	2.665 ± 0.432	2.00E–04 ± 1.00E–04	1.43E–05 ± 2.63E–06
WC–Hastelloy	2.003 ± 0.020	1.00E–04 ± 0	1.08E–05 ± 1.11E–06
Cr <sub>3</sub> C <sub>2</sub> –NiCr	11.526 ± 0.462	9.00E–04 ± 1.00E–04	6.25E–05 ± 2.50E–06
(Ti,Mo)(C,N)–NiCo	7.220 ± 0.251	5.00E–04 ± 0	3.91E–05 ± 1.36E–06
NiCrSiB	47.970 ± 0.978	3.60E–03 ± 1.00E–04	2.60E–04 ± 5.31E–06
AISI 316L	134.362 ± 12.274	1.08E–02 ± 9.00E–04	7.29E–04 ± 6.00E–05
Cr <sub>2</sub> O <sub>3</sub>	18.183 ± 0.813	1.50E–03 ± 0	9.86E–05 ± 4.41E–06
Hardened steel	73.305 ± 8.567	5.60E–03 ± 5.00E–04	3.98E–04 ± 4.64E–05
Hard chrome	35.308 ± 3.412	2.00E–03 ± 3.00E–04	1.92E–04 ± 1.85E–05

**Fig. 10** Worn surface of WC–Co coating after wet abrasion test

chloride solution under sliding wear, mechanical and electrochemical damage phenomena were observed to differing degrees under different conditions. It was shown [37] that wear-corrosion resistance is influenced by two concomitant factors, i.e., coating hardness and toughness (related to the ceramic constituent and to the ceramic/metallic ratio) and metal matrix corrosion resistance. According to the experimental conditions used, mechanical properties can prevail over corrosion resistance or vice versa. In agreement with our results, among WC-based systems, the chromium-containing coatings showed the lowest tribocorrosion rate. The tribocorrosion behavior of WC-based coatings with different microstructures was studied by Souza et al. [38] in a sodium chloride solution under erosive conditions. The synergy effect of wear and corrosion was studied, and the influence of coating microhardness, toughness, and Young's modulus described in the study confirmed our observations.

The same wear mechanism, microgrinding and polishing, was observed for the (Ti,Mo)(C,N)–NiCo coating. The

**Fig. 11** Worn surface of (Ti,Mo)(C,N)–NiCo coating after wet abrasion test

worn surface was very smooth, without signs of cracks or brittle delamination. The small rupture on the hard phase-matrix boundary that could later lead to pullout of the hard phase can be seen in the detailed SEM image in Fig. 11.

The worn surface of the Cr<sub>3</sub>C<sub>2</sub>–NiCr coating differed from the surfaces of the previous hardmetal coatings by the existence of a tribofilm. For the pin-on-disk test, the conditions and mechanism of tribofilm creation for hardmetal coatings was described by Bolelli et al. [9], according to whom the tribofilm consists of plastically deformed matrix material and wear debris and/or in a surface chemical alteration of the coating. In the case of sufficient cohesion to the surface and to itself, the tribofilm is beneficial for the coating's wear resistance.

The other two HVOF coatings, metallic NiCrSiB and AISI 316L, underwent wear by a similar mechanism. Because they both did not contain hard phases, which could influence the wear mechanism and decrease the wear rate, their wear loss was high. The wear mechanism was

identified to involve cutting and ploughing. No embedding of abrasive particles in AISI 316L was observed. The presence of water and a significantly lower abrasive particle size made the process of wear milder compared with the process occurring in the dry abrasion wear test.

The influence of corrosion on wear results of these two metallic coatings is not clear. EDX analyses of worn surfaces did not prove the presence of corrosive products, but the possibility of their continuous formation and removal by abrasive particles cannot be excluded.

The wear mechanism of the ceramic plasma-sprayed  $\text{Cr}_2\text{O}_3$  coating was similar to that of dry abrasion. The wear loss was characterized by brittle cracking of coating fragments due to the lower intersplat cohesion and adhesion and the presence of shrinkage cracks, together with fatigue of abrasive particles.

The wet slurry abrasion resistance of the above-mentioned coatings is described in detail by Nohava et al. [39].

The ranking of WC-based coatings differed from that obtained in the dry sand rubber wheel test due to the given corrosive conditions. The conditions of the dry sand/rubber wheel test—the bigger abrasive particles and lack of water compare to the slurry consisting from small abrasive particles and water—were propitious for wear resistance in AISI 316L probably due to the embedding of abrasive particles, but not for NiCrSiB due to the low cohesion and not for  $\text{Cr}_2\text{O}_3$  due to the plasma-sprayed coating brittleness.

### 3.3 Pin-on-Disk Test

The results of the pin-on-disk wear test are summarized in Table 7. Coating wear was not measured for the case of the steel pin, which is much softer than the coatings. According to Bolelli et al. [6], material buildup on the coating surface can be expected. In this case, only coefficients of

friction were measured. For the  $\text{Al}_2\text{O}_3$  pin, the hardness of which is comparable with that of the carbides in the hardmetal coatings and the  $\text{Cr}_2\text{O}_3$  coating, the wear track area was measured and the wear rate calculated. The volume loss for the most resistant coatings, the WC-based hardmetal coatings and the  $\text{Cr}_2\text{O}_3$  coating, was too small to be measured by the available equipment (profilometer Hommel Tester 1000). The ranking of the measurement results matched the expectations: the most resistant WC-based coatings (for which measurements could not be made) and the  $\text{Cr}_2\text{O}_3$  coating were followed by the other HVOF coatings, (Ti,Mo)(C,N)–NiCo and  $\text{Cr}_3\text{C}_2$ –NiCr. The next were hardened steel, the NiCrSiB coating, and the AISI 316L coating, and the worst results were obtained for the hard chrome coatings. With respect to coating hardness (Table 3), the ranking of the pin-on-disk test results matched that of the HR15N results with the exception of hardened steel and hard chrome. The hardened steel exhibited higher wear resistance, whereas hard chrome was the worst of the evaluated coatings, despite its high hardness. The wear resistance of the coatings is determined also by the properties of wear debris. The wear mechanism, described below, has to be taken into account concerning the wear rate. To the high wear of hard chrome, the hard released wear debris as well as the lower coating thickness can contribute. Because the thickness of the hard chrome coating was lower than the other coating thicknesses due to the manufacturing process used, the high measured wear track area could also have been caused by plastic deformation of the substrate material.

The mechanism of wear was studied by SEM evaluation for all tests. The major wear mechanism of the HVOF hardmetal coating was connected with the gradual primary loss of the metal matrix from the areas between the hard particles of the coating, leading to the weakening of the bonding of the hard phase particles and their pullout from the coating surface. The design of the CSM Tribometer does not allow the wear debris to fall off naturally; it is trapped in the wear track and serves as an abrasive medium. Then the mechanism of wear changes from sliding to abrasive wear [24, 40]. The wear track of WC–17%Co can be seen in Fig. 12. An area of the wear track bottom looked very similar to the unworn polished surface, whereas the sides of the wear track showed sharp carbides protruding from the worn matrix. In the article by Bolelli et al. [6], the wear mechanism of the cermet coatings is described as the contact between the pin and the coating's carbides, which protrude slightly from the matrix due to grinding. These conditions lead to very slight wear only. In this case, the COF is determined by the friction of WC grains with  $\text{Al}_2\text{O}_3$ , and the matrix material does not play such a significant role. This theory was confirmed by the measured experimental data.

**Table 7** Results of pin-on-disk test

Coating	Coeff. of wear resistance $K_{\text{abr}}$ ( $\text{mm}^3/\text{Nm}$ )	COF for $\text{Al}_2\text{O}_3$ ball	COF for steel ball
WC–Co	–	$0.369 \pm 0.008$	$0.780 \pm 0.011$
WC–CoCr	–	$0.398 \pm 0.009$	$0.757 \pm 0.033$
WC–Hastelloy	–	$0.382 \pm 0.011$	$0.811 \pm 0.008$
$\text{Cr}_3\text{C}_2$ –NiCr	$5.5\text{E}-6$	$0.549 \pm 0.008$	$0.717 \pm 0.093$
(Ti)(Mo)(C,N)–NiCo	$0.35\text{E}-6$	$0.653 \pm 0.016$	$0.529 \pm 0.011$
NiCrSiB	$65\text{E}-6$	$0.645 \pm 0.026$	$0.622 \pm 0.024$
AISI 316L	$182\text{E}-6$	$0.644 \pm 0.021$	$0.638 \pm 0.030$
$\text{Cr}_2\text{O}_3$	–	$0.350 \pm 0.032$	$0.567 \pm 0.015$
Hardened steel	$6.2\text{E}-6$	$0.568 \pm 0.008$	–
Hard chrome	$277\text{E}-6$	$0.704 \pm 0.023$	–

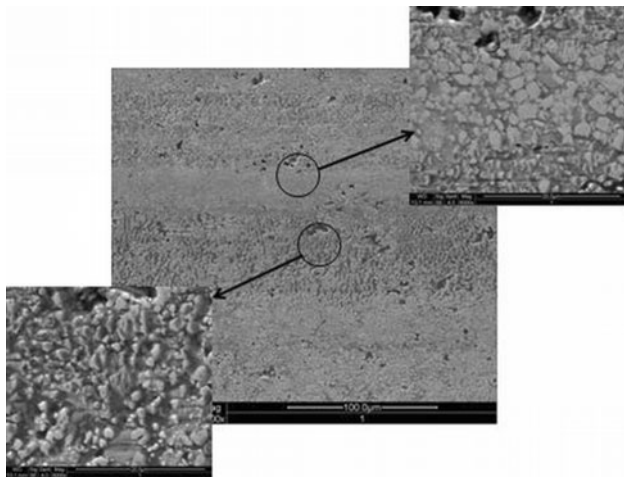


**Fig. 12** WC–Co coating's pin-on-disk wear track

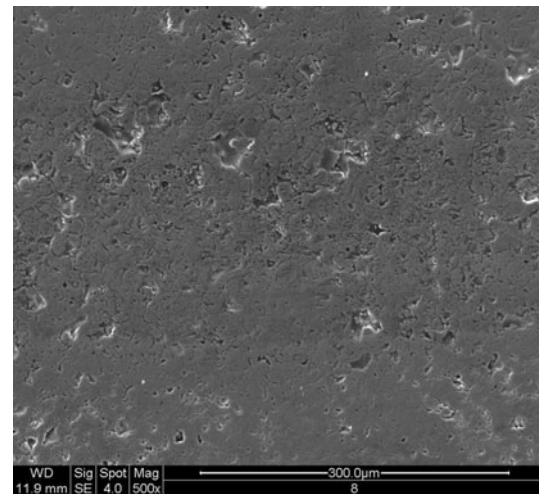


**Fig. 14** Cr<sub>2</sub>O<sub>3</sub> coating's pin-on-disk wear track

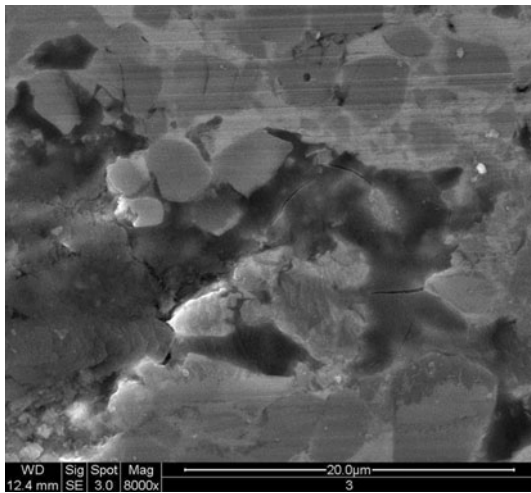


**Fig. 13** Cr<sub>3</sub>C<sub>2</sub>–NiCr coating's pin-on-disk wear track

In the case of the Cr<sub>3</sub>C<sub>2</sub>-based coatings, due to the lower fracture toughness, a higher amount of carbides and also larger wear debris particles were pulled out. In the wear track, cracks could be observed in the matrix near the carbides; these cracks could cause carbide pullouts from the matrix (Fig. 13). A poor bonding of Cr<sub>3</sub>C<sub>2</sub> grains into the metallic matrix is typically found in coatings of this composition [41]. In the article by Bolelli et al. [6], the formation of the tribofilm consisting of the oxidized, plastically deformed matrix was recognized, and could also be expected, even though it was not proven in this study.

Besides the above-mentioned effects, signs of plastic deformation and loss of larger splat pieces were observed for the (Ti,Mo)(C,N)–NiCo hardmetal coating.

The metallic HVOF-sprayed coatings showed a much higher extent of plastic deformation accompanied by loss of splat cohesion, especially on the wear track edges.

A completely different wear mechanism was observed for the brittle plasma-sprayed Cr<sub>2</sub>O<sub>3</sub> coating. Formation of cracks in the wear track was followed by pullout of coating fragments (Fig. 14). The principle of the pin-on-disk test is based on repeated loading, which caused fatigue stress in the hard and brittle Cr<sub>2</sub>O<sub>3</sub> coating and led to formation of fatigue cracks, which were responsible for the wear.

Even though the wear of the hardmetal coatings was not measurable after the test performed with a steel ball, the appearance of the tracks was found different from the mechanism of wear for the tests with the Al<sub>2</sub>O<sub>3</sub> ball. In the case of hard coatings, ball material was transferred to the coating surface, creating microwelds between pin material and matrix. The microwelds caused larger coating parts to be pulled out; this was observed mainly in the Cr<sub>3</sub>C<sub>2</sub>–NiCr coating. Besides having an effect on the wear mechanism, this influenced the measured COF.

The measured coefficient of friction values for two kinds of pin material are summarized in Table 7. The measurements obtained with the Al<sub>2</sub>O<sub>3</sub> ball were the lowest in the case of the analogous material—the Cr<sub>2</sub>O<sub>3</sub> coating. The next group of materials with low friction coefficients was formed by WC-based coatings. This was due to the wear mechanism described above. Contact between the Al<sub>2</sub>O<sub>3</sub> pin and the coating surface was assured by ground WC carbides. For the other hardmetal coatings, the value of coefficient of friction was higher, probably due to the influence of the carbides released from the matrix.

The hardmetal HVOF-sprayed coatings' COFs and coefficient of wear resistance measurements using an Al<sub>2</sub>O<sub>3</sub> mating part are also described in the literature [29]. The dependence of COF on sliding speed and temperature was measured. Compared with the results at similar conditions, the values of COF measured in our study were



slightly lower, but on the same order of magnitude. The only exception was the COF of the (Ti,Mo)(C,N)-based coating. The same could be said about the coefficients of wear resistance.

The COFs measured using the steel ball were higher than those measured using the alumina ball for all hard-metal coatings except (Ti,Mo)(C,N)-NiCo. For the metal coatings, the measured COF was slightly lower. According to Bolelli et al. [6], the deformed wear debris from the steel pin is transferred to the coating surface, where it creates a tribofilm that influences the COF.

The results of COF measurement can also be influenced by tribooxidation. The mechanism of tribooxidation is described by Bhushan [24], but it was not studied in this study.

### 3.4 Erosion Wear Test

The erosion wear test results for three angles of particle impingement are summarized in Fig. 15. Most of the coatings were more wear-resistant when the particle impingement angle was low. This fact results from the primary coatings' use as coatings resistant to abrasive wear. A perpendicular particle impingement caused greater damage in more brittle coatings such as the plasma-sprayed  $\text{Cr}_2\text{O}_3$  coating, the HVOF-sprayed  $\text{Cr}_3\text{C}_2$ -NiCr and (Ti,Mo)(C,N)-NiCo hardmetal coatings, and the metallic NiCrSiB coating, with the disadvantage of having low cohesion. The surfaces with conventional surface treatments, the hard chrome coatings and the hardened steel surface, showed very good results in the erosion wear test.

For a small impingement angle, the mechanism of wear was similar to that observed for abrasive wear. In the case of perpendicular impingement, the worn surfaces differed according to their microstructures.

The WC-CoCr coating after the erosion wear test is shown in Fig. 16. The perpendicular impingement

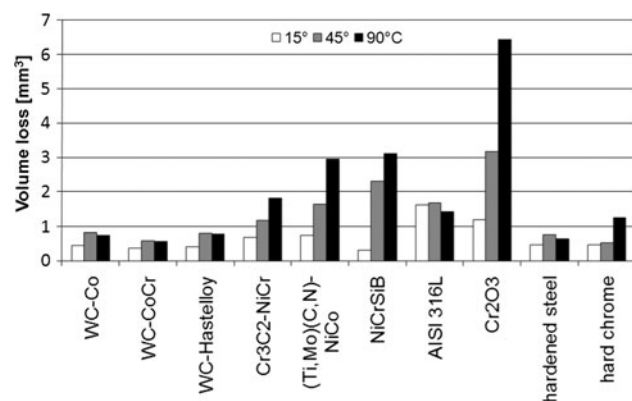


**Fig. 15** Erosion wear test results

(Fig. 16a) caused the creation of pinholes from the impact of sharp-edged particles. There was no evidence of cracking in the matrix or carbides. Figure 16b shows the surface after 45° impingement. Except for pinholes, a certain amount of

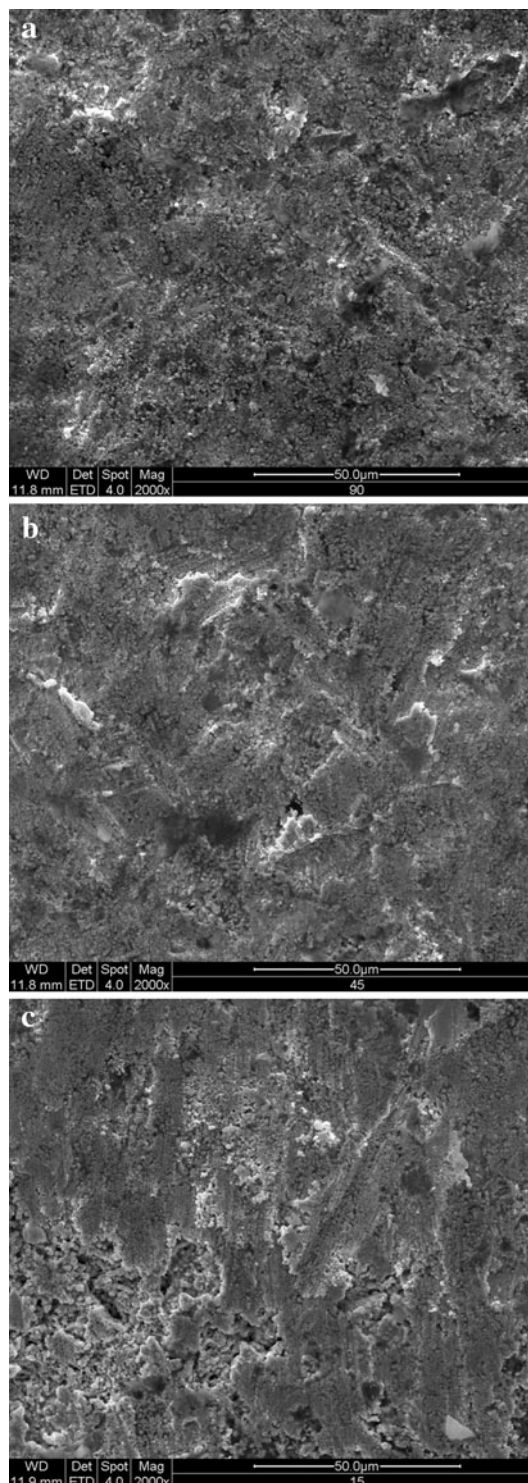


**Fig. 16** WC-CoCr coating surface after erosion wear test at a particle impingement angle of **a** 90°, **b** 45°, and **c** 15°



ploughing was found. The ploughing mechanism was observed to dominate when the impingement angle was low (Fig. 16c). The carbide pullout mechanism was not observed for any of the hardmetal coatings. On the contrary, the carbides seemed to be pushed into the matrix. Unlike in the HVOF alloy coatings, in the WC–CoCr coating, the presence of carbides decreased the amount of plastic deformation as well as the material loss.

The surfaces of the HVOF alloy coatings (AISI 316L, NiCrSiB) after the perpendicular erosion test did not contain any pinholes as in the hardmetal coatings. The surface was formed from individual splats with only small indications of particle impingement (Fig. 17a). This fact, together with signs of subsurface detachment (Fig. 18), determined the mechanism of material loss to be release of entire splats. Lowering of the impingement angle resulted in an increase in the percentage of plastic deformation and the amount of tracks from abrasive cutting and ploughing (Fig. 17b, c).

The appearance of the ceramic plasma-sprayed  $\text{Cr}_2\text{O}_3$  coating surface (Fig. 19) after  $90^\circ$  and  $45^\circ$  impingement and the high material loss indicated that the main wear mechanism was also complete splat release. In the case of  $15^\circ$  impingement, the coating surface appeared to be gently ground; shallow wear tracks from abrasive cutting were observed.

The results are in an agreement with the results of other erosion studies. As for other WC-based hardmetal coatings [42], the three investigated coatings in this study showed a maximum wear rate at  $45^\circ$ . The study of the effect of impingement angle on erosion-corrosion behavior of HVOF WC-based coatings [43] demonstrates the greater vulnerability of the hardmetal coatings to solid/liquid streams impinging at higher angles, and this trend appears to exist over a range of solid loads.

Legoux et al. [44] identified the three main factors influencing the HVOF coating erosion wear resistance in the case of perpendicular impingement to be local hardness, matrix properties, and splat debonding. In an earlier study [45], the erosion resistance of HVOF WC–Co–Cr coatings was studied under different erosion conditions. The influence of angle of impingement is explained by an amount of energy that is transferred to the material during impact. In the case of a high impact angle, the brittle material is more prone to fracture, since no other type of energy release mechanism can be activated. At a lower impact angle, other types of mechanisms such as material cutting and ploughing take part. Under these conditions, ductile materials are more easily deformed and thus will have a lower erosion resistance [23]. The same conclusion was made by Hussainova et al. [46], but for hardmetals prepared by conventional powder metallurgy sintering, not thermally sprayed hardmetal coatings.

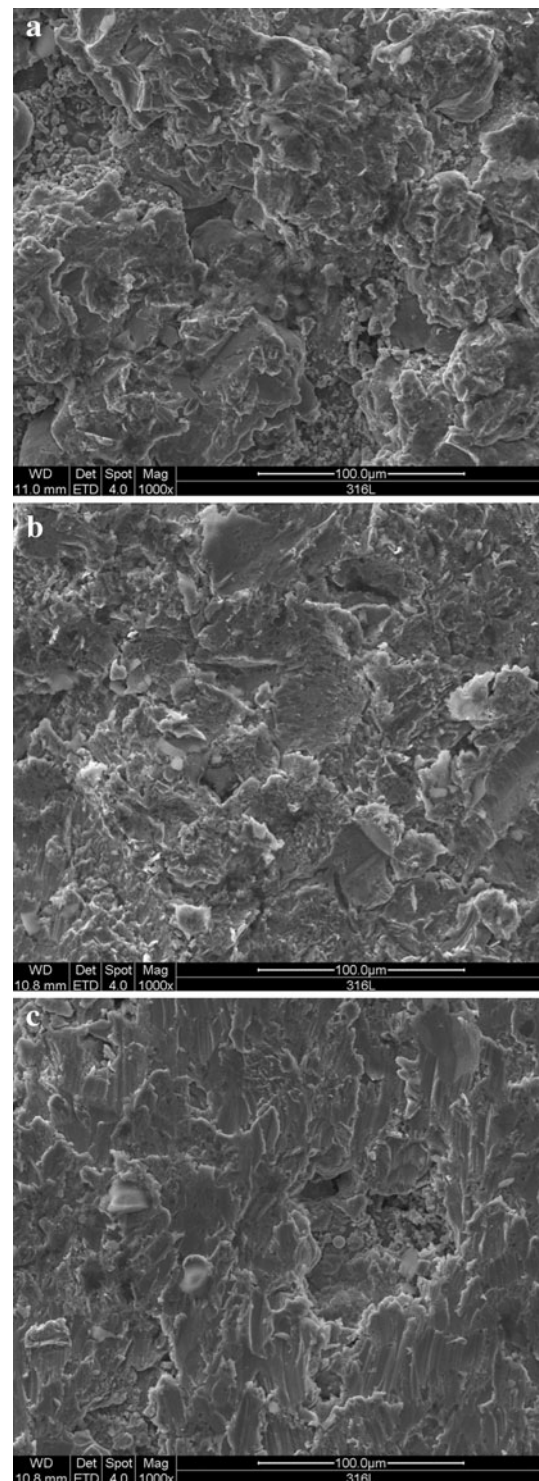


**Fig. 17** AISI 316L coating surfaces after erosion wear test at a particle impingement angle of **a**  $90^\circ$ , **b**  $45^\circ$ , and **c**  $15^\circ$

#### 4 Conclusions

The tribological behavior of seven thermally sprayed coatings was evaluated by four different wear test methods.

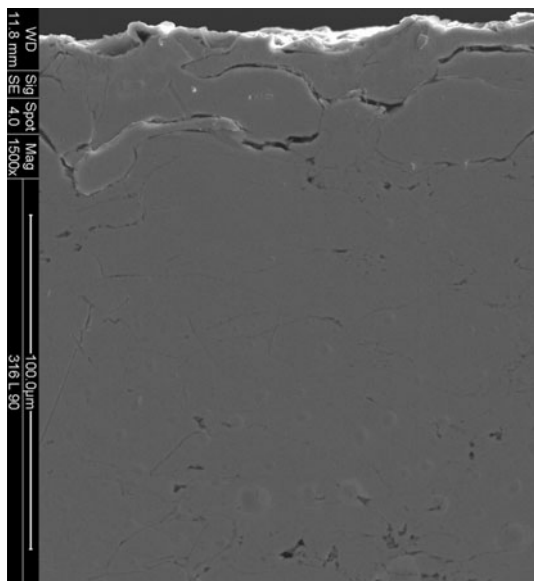


**Fig. 18** Cross-section of AISI 316L coating after erosion wear test at a particle impingement angle of  $90^\circ$

The wear resistance, mechanisms of wear and coefficient of friction were measured and compared with the wear resistance of electrolytic hard chrome and surface-hardened steel. In all tests, the HVOF-sprayed hardmetal coatings exhibited superior properties and can be recommended as a replacement for traditional surface treatments. The plasma-sprayed ceramic coating  $\text{Cr}_2\text{O}_3$ , due to its tendency to exhibit brittle cracking, can only be recommended for sliding wear conditions. The tested metallic HVOF-sprayed coatings, NiCrSiB and AISI 316L, did not have sufficient wear resistance compared with that of traditional surface treatment and should not be used under more demanding conditions. The relatively high wear resistance of the AISI 316L coating in the DSRW abrasion test is caused by embedding of the abrasive particles to the coating surface. This effect can not be ensured for all possible coating applications and without it the coating has a very low wear resistance, as it was proved in wet abrasion wear test.

The mechanism of wear was similar for all tests performed. In the case of hardmetal coatings, a main wear mechanism was found to be the gradual loss of matrix material, followed by weakening of the hard particle bonds and pullout from the coating surface. In the case of ceramic coatings, material loss was realized by brittle cracking, enhanced by fatigue stress. For the metallic coatings, material loss was realized mainly by scratching and ploughing, with the exception of erosion wear in the case of perpendicular particle impact, where, for the AISI 316L coating, subsurface cracking appeared and the entire splats were detached from the surface.

The relationship between the basic properties, hardness, and fracture toughness of the coatings cannot be directly

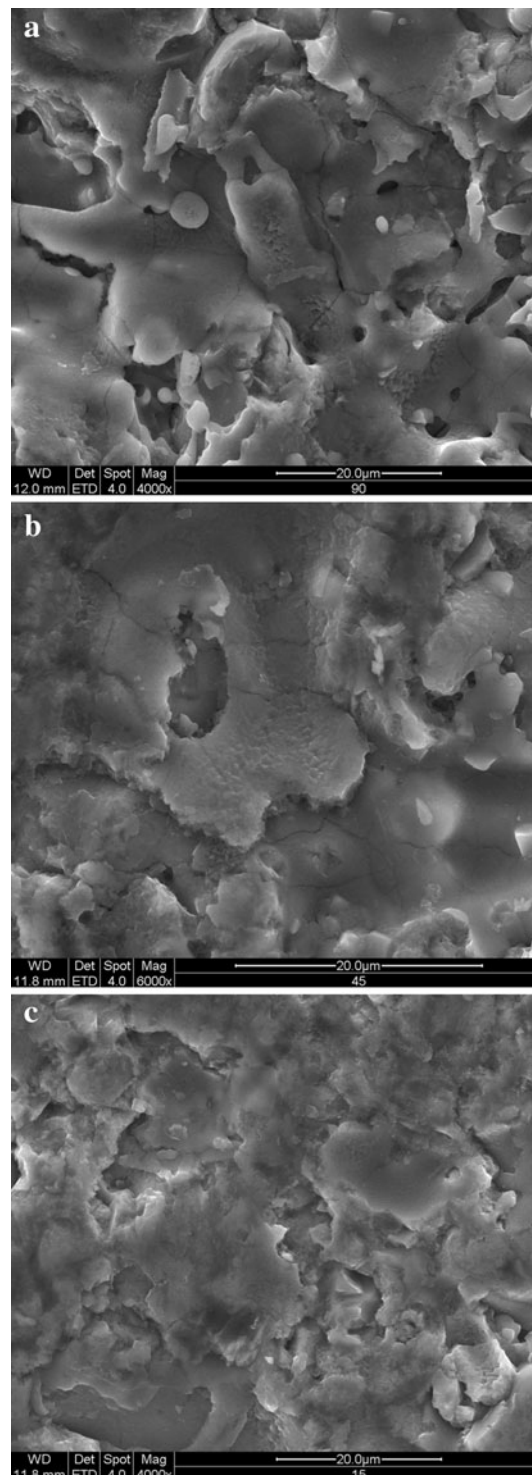


**Fig. 19**  $\text{Cr}_2\text{O}_3$  coating surface after erosion wear test at a particle impingement angle of **a**  $90^\circ$ , **b**  $45^\circ$ , and **c**  $15^\circ$

correlated with the wear test results. Based on the measurement, the surface hardness appeared to be more related to the dry and slurry abrasion wear results than the microhardness. The hardness was more important in the wet slurry abrasion test, where the mechanism of wear was

purely abrasive, whereas the brittleness played a role in the case of the DSRW test, where indentation also occurred. In the pin-on-disk test, besides the hardness, the ability of the coating material to resist cracking was also found to be important. Not only the coating material itself, but also its interaction with the mating part material played an important role. The erosion wear test combined the requirements on the materials' properties according to the particle impingement angle. For perpendicular particle impact, the brittle coatings as well as coatings with low cohesion had been the less resistant. For low impact angle, no simple relationship between hardness or fracture toughness and wear resistance was found. In that case, the combination of both properties is decisive.

**Acknowledgments** This study was supported by the Ministry of Industry and Trade of the Czech Republic within the framework of the program TANDEM no. FT-TA5/07. The erosion wear measurement was done in collaboration with ATG Ltd., Czech Republic.

## References

- Dayan, A.D., Paine, A.J.: Mechanisms of chromium toxicity, carcinogenicity and allergenicity: review of the literature from 1985 to 2000. *Hum. Exp. Toxicol.* **20**, 439–451 (2001)
- Von Burg, R., Liu, D.: Chromium and hexavalent chromium. *J Appl. Toxicol.* **13**, 225–230 (1993)
- Costa, M.: Toxicity and carcinogenicity of Cr<sup>(VI)</sup> in animal models and humans. *Crit. Rev. Toxicol.* **27**, 431–442 (1997)
- Directive 2002/95/EC of the European Parliament and of the Council on the restriction of the use of certain hazardous substances in electrical and electronic equipment. *Off. J. Eur. Union* **1**, 27, pp. 19–37 (2003)
- Pawlowski, L.: *Science and Engineering of Thermal Spray Coatings*, 2nd edn. Wiley, Chichester (2008)
- Bolelli, G., Cannillo, V., Lusvardi, L., Manfredini, T.: Wear behavior of thermally sprayed ceramic oxide coatings. *Wear* **261**, 1298–1315 (2006)
- Picas, J.A., Forn, A., Matthäus, G.: HVOF coatings as an alternative to hard chrome for pistons and valves. *Wear* **261**, 477–484 (2006)
- Kirsten, A., Oechsle, M., Moll, R. F.: Carbide containing materials for hard chromium replacement by HVOF-spraying. In: *Proceeding of the International Thermal Spray Conference ITSC 2005*, Basel, 2–4 May 2005, pp. 957–962. DVS-Verlag, Basel, Switzerland, Düsseldorf, (2005). CD (ISBN 3-87155-793-5)
- Bolelli, G., Cannillo, V., Lusvardi, L., Soragni, E., Loreto, A., Valente, T.: A comprehensive characterization of industrially manufactured hard chrome platings and of thermally sprayed alternatives. In: *Proceeding of the International Thermal Spray Conference ITSC 2005*, Basel, 2–4 May 2005, pp. 1456–1461. DVS-Verlag, Basel, Switzerland, Düsseldorf (2005). CD (ISBN 3-87155-793-5)
- Guilemany, J.M., Espallargas, N., Suegama, P.H., Benedetti, A.V., Fernandez, J.: High-velocity oxyfuel Cr<sub>3</sub>C<sub>2</sub>-NiCr replacing hard chromium coatings. *J. Therm. Spray Technol.* **14**, 335–341 (2005)
- Wank, A., Schwenk, A., Wielage, B., Grund, T., Friesen, E., Pokhmurska, H.: Behavior of thermally sprayed wear protective coatings exposed to different abrasive wear conditions in comparison to hard chromium platings. In: *Conf. Proc. Int. Thermal Spray Conference & Exhibition ITSC 2007*, 14–16 May 2007, Beijing, China, pp. 1011–1016. ASM International, Materials Park, Ohio, USA (2007)
- Sartwell, B.D.: Thermal spray copatings replace hard chrome plating on aircraft components. *AMPTIAC Newslett.* **3**, 1–7 (1999)
- Lekatou, A., Zois, D., Grimanelis, D.: Corrosion properties of HVOF cermet coatings with bond coats in an aqueous chloride environment. *Thin Solid Films* **516**, 5700–5705 (2008)
- Bolelli, G., Cannillo, V., Giovanardi, R., Lusvardi, L.: Electrochemical comparison between corrosion resistance of some thermally sprayed coatings. *Int. J. Surf. Sci. Eng.* **2**, 222–239 (2008)
- Breitsameter, M.: Thermal spraying versus hard chrome plating. *Mater. Australas.* **32**, 11–13 (2000)
- Ponton, C.B., Rawlings, R.D.: Vickers indentation fracture toughness test. Part 1. *Mater. Sci. Technol.* **5**, 865–872 (1989)
- Ponton, C.B., Rawlings, R.D.: Vickers indentation fracture toughness test. Part 2. *Mater. Sci. Technol.* **5**, 961–976 (1989)
- Houdková, Š., Enžl, R., Zahálka, F., Bláhová, O.: The indentation tests for evaluation of HVOF coatings' mechanical properties. In: *Conf. Proc. Int. Thermal Spray Conference & Exhibition ITSC 2005*, 2–4 May 2005, pp. 1521–1525. DVS-Verlag, Basel, Switzerland, Düsseldorf (2005). CD (ISBN 3-87155-793-5)
- Lawn, B.R., Fuller, E.R.: Equilibrium penny-like cracks in indentation fracture. *J. Mater. Sci.* **10**, 2016–2024 (1975)
- Kašparová, M., Zahálka, F., Houdková, Š., Ctibor, P.: Abrasive wear of WC–NiMoCrFeCo thermally sprayed coatings in dependence on different type of abrasive sands. *Kovove Mater.* **48**, 73–85 (2010)
- Houdková, Š., Zahálka, F., Kašparová, M., Berger, L.-M.: Tribological behavior of thermally sprayed coatings at elevated temperatures. In: *Conf. Proc. Int. Thermal Spray Conference & Exhibition ITSC 2008*, 2–4 June 2008, Maastricht, The Netherlands, pp. 1485–1590. ASM International, Materials Park, Ohio, USA (2008)
- Berger, L.-M., Martens, S., Kleemann, C., Enzl, R., Schulz, I., Zieris, R.: Investigation of rolling contact fatigue of HVOF-sprayed hardmetal coatings in dry conditions. *J. Therm. Spray Technol.* (Submitted)
- Bayer, R.G.: *Mechanical Wear Prediction and Prevention*. Marcel Dekker, Inc., New York, USA (1994)
- Bhushan, B.: *Introduction to Tribology*. Wiley, New York, USA (2002)
- Kleis, I., Kulu, P.: *Solid Particle Erosion: Occurrence, Prediction and Control*. Springer, London (2008)
- Kašparová, M., Zahálka, F., Houdková, Š., Ctibor, P.: Properties of HVOF sprayed coatings influenced by laser after-treatment. In: *Proceedings of International conference MATRIB 2007*, 21–23 June 2007, Croatia, ISBN 978-953-7040-12-3, (2007)
- Miguel, J.M., Guilemany, J.M., Vizcaino, S.: Tribological study of NiCrBSi coating obtained by different process. *Tribol. Int.* **36**, 181–187 (2003)
- Bolelli, G., Cannillo, V., Lusvardi, L., Riccò, S.: Mechanical and tribological properties of electrolytic hard chrome and HVOF-sprayed coatings. *Surface Coat. Technol.* **200**, 2995–3009 (2006)
- Berger, L.-M., Saaro, S., Woydt, M.: Reib-/Gleitverschleiß von thermisch gespritzten Hartmetallschichten, *Jahrbuch Oberflächentechnik* **63**, ISBN 978-3-87480-234-5, pp. 242–267 (2007)
- Berger, L.-M., Thiele, S., Vuoristo, P., Mäntylä, T., Keller, H., Proß, E., Scholl, R.: Titanium carbide-based powders and coatings—compositions, processability and properties. In: *Proc. Int. Thermal Spray Conf. 2002*, pp. 727–732. DVS-Verlag, Lugschneider, Düsseldorf (2002)

31. Berger, L.-M., Zimmermann, S., Keller, H., Schwier, G., Thiele, S., Nebelung, M., Enzl, R.: Microstructure and properties of HVOF-sprayed TiC-based coatings. In: Moreau, C., Marple, B. (eds.) *Thermal Spray 2003: Advancing the Science and Applying the Technology*, pp. 793–799. ASM Int, Material Park/Ohio (2003)
32. Berger, L.-M., Woydt, M., Zimmermann, S., Keller, H., Schwier, G., Enzl, R., Thiele, S.: Tribological behavior of HVOF-sprayed Cr<sub>3</sub>C<sub>2</sub>-NiCr and TiC-based coatings under high-temperature dry sliding conditions. In: *Conf. Proc. Int. Thermal Spray Conference & Exhibition ITSC 2004*, 10–12 May 2004, p. 10. DVS-Verlag, Osaka, Japan, Düsseldorf (2004). CD (ISBN 3-87155-792-7)
33. Zieris, R., Berger, L.-M., Schulz, I., Martens, S., Enzl, R.: Investigation of ceramic and hardmetal coatings in an oscillating sliding wear test. In: *Conf. Proc. Int. Thermal Spray Conference & Exhibition ITSC 2005*, 2–4 May 2005, pp. 860–867. DVS-Verlag, Basel, Switzerland, Düsseldorf (2005). CD (ISBN 3-87155-793-5)
34. Yang, Q., Senda, T., Ohmori, A.: Effect of carbide grain size on microstructure and sliding wear behavior of HVOF-sprayed WC–12%Co coatings. *Wear* **254**, 23–34 (2003)
35. Chivavibul, P., Watanabe, M., Kuroda, S., Shinoda, K.: Effect of carbide size and Co content on the microstructure and mechanical properties of HVOF-sprayed WC–Co coatings. *Surface Coat. Technol.* **202**, 509–521 (2007)
36. Berger, L.-M., Eitmayer, P., Vuoristo, P., Mäntylä, T., Kunert, W.: Microstructure and properties of WC–10%Co–4%Cr spray powders and coatings. I. Powder characterization. *J. Therm. Spray Technol.* **10**, 311–325 (2001)
37. Fedrizzi, L., Valentinelli, L., Rossi, S., Segna, S.: Tribocorrosion behavior of HVOF cermet coatings. *Corros. Sci.* **49**, 2781–2799 (2007)
38. Souza, V.A.D., Neville, A.: Aspects of microstructure on the synergy and overall material loss of thermal spray coatings in erosion-corrosion environments. *Wear* **263**, 339–346 (2007)
39. Nohava, J., Enzl, R., Zahálka, F., Foucher, C.: Fractographic approach to wear mechanism of selected thermally sprayed coatings. In: *Conf. Proc. Int. Thermal Spray Conference & Exhibition ITSC 2005*, 2–4 May 2005, pp. 875–880. DVS-Verlag, Basel, Switzerland, Düsseldorf (2005). CD (ISBN 3-87155-793-5)
40. Houdková, Š., Zahálka, F., Kašparová, M.: The influence of thermally sprayed coatings microstructure on their mechanical and tribological characteristics. *Mater. Sci. Forum* **567–568**, 229–232 (2007)
41. Berger, L.-M.: Hardmetals as thermal spray coatings. *Powder Metall.* **50**, 205–214 (2007)
42. Berger, L.-M., Saaro, S., Naumann, T., Wiener, M., Weihnacht, V., Thiele, S., Suchánek, J.: Microstructure and properties of HVOF-sprayed chromium alloyed WC–Co and WC–Ni coatings. *Surface Coat. Technol.* **202**, 4417–4421 (2008)
43. Hodgkiess, T., Perry, J.M., Neville, A.: Effect of angle of impingement on erosion-corrosion behaviour of a WC–Co–Cr HVOF sprayed coating. In: *Conf. Proc. Int. Thermal Spray Conference & Exhibition ITSC 2005*, 2–4 May 2005, pp. 715–719. DVS-Verlag, Basel, Switzerland, Düsseldorf (2005). CD (ISBN 3-87155-793-5)
44. Legoux, J.-G., Bouaricha, S., Marcoux, P.: Abrasion and erosion of WC and CrC cermet coatings. In: *Conf. Proc. Int. Thermal Spray Conference & Exhibition ITSC 2004*, 10–12 May 2004. DVS-Verlag, Osaka, Japan, Düsseldorf (2004). CD (ISBN 3-87155-792-7)
45. Legoux, J.-G., Arsenaault, B., Hawthorne, H., Immarigeon, J.-P.: Erosion behavior of WC–10Co–4Cr HVOF coatings. In: Moreau, C., Marple, B. (eds.) *Thermal Spray 2003: Advancing the Science and Applying the Technology*, pp. 405–410. ASM Int, Material Park/Ohio (2003)
46. Hussainova, I., Pirso, J., Antonov, M., Juhani, K., Letunovits, S.: Erosion and abrasion of chromium carbide based cermets produced by different methods. *Wear* **263**, 905–911 (2007)